

# 1           **Experimental Study on the Ignition Characteristics of Cellulose,** 2                           **Hemicellulose, Lignin and Their Mixtures**

3                           Wenhan Cao<sup>a</sup>, Jun Li<sup>a\*</sup>, Teresa Martí-Rosselló<sup>a</sup>, Xiaolei Zhang<sup>b</sup>

4           <sup>a</sup>*Department of Chemical and Process Engineering, University of Strathclyde, Glasgow, G1 1XJ, UK*

5           <sup>b</sup>*School of Mechanical and Aerospace Engineering, Queen's University of Belfast, BT9 5AH, UK*

## 6           **Abstract**

7  
8           Ignition behaviour of biomass is an essential knowledge for plant design and process control  
9           of biomass combustion. Understanding of ignition characteristics of its main chemical  
10           components, i.e. cellulose, hemicellulose, lignin and their mixtures will allow the further  
11           investigation of ignition behaviour of a wider range of biomass feedstock. This paper  
12           experimentally investigates the influences of interactions among cellulose, hemicellulose and  
13           lignin on the ignition behaviour of biomass by thermogravimetric analysis. Thermal  
14           properties of an artificial biomass, consisting of a mixture of the three components will be  
15           studied and compared to that of natural biomass in atmospheres of air and nitrogen in terms  
16           of their ignition behaviour. The results showed that the identified ignition temperatures of  
17           cellulose, hemicellulose and lignin are 410°C, 370°C and 405°C, respectively. It has been  
18           found that the influence of their interactions on the ignition behaviour of mixtures is  
19           insignificant, indicating that the ignition behaviour of various biomass feedstock could be  
20           predicted with high accuracy if the mass fractions of cellulose, hemicellulose and lignin are  
21           known. While the deficiencies of the determined mutual interactions would be further  
22           improved by the analytical results of the activation energies of cellulose, hemicellulose,  
23           lignin, their mixtures as well as natural and artificial biomass in air conditions.

24           **Keywords:** *biomass; ignition temperature; kinetics; cellulose; hemicellulose; lignin*  
25

---

Corresponding author. Tel.: 01415482393  
E-mail address: jun.li@strath.ac.uk

## 26 1. Introduction

27 Biomass is considered to be a carbon-neutral and renewable fuel, which holds a great  
28 potential to act as an alternative energy resource to address the challenging of global warming  
29 and worldwide energy crisis <sup>[1]</sup>. Compared with other thermal conversion technologies, direct  
30 combustion is known as the most efficient approach of biomass utilization for heat and power  
31 generation <sup>[2]</sup>. However, firing biomass in modified fuel boilers or co-firing biomass with  
32 coal in existing coal-fired boilers is a complicate process <sup>[3]</sup>, an optimal operation of the  
33 biomass combustion process requires essential knowledge of its combustion performances,  
34 especially flame properties and ignition behaviour. Ignition plays a crucial role in  
35 combustion, having a significant impact on the boiler operation, energy efficiency, as well as  
36 in the gas emissions <sup>[4]</sup>. Ignition temperature and ignition delay time are known as two  
37 important operational indicators to initialise combustion processes <sup>[5]</sup>. Most ignition studies  
38 were conducted to control and minimise the self-ignition risks during transport, handling and  
39 processing biomass materials <sup>[6]</sup>, but ignition mechanism with regard to improvement of  
40 combustion performances are rarely reported.

41 Previous studies have attempted to investigate the ignition behaviour of biomass with the aim  
42 of improving and making the biomass co-firing performance comparable with that of coal.  
43 Rianza et al. <sup>[7]</sup> reported that ignition behaviour of coal could be improved by adding biomass  
44 in an air or oxy-firing atmosphere, especially remarkable for high rank coals. Shan et al. <sup>[8]</sup>  
45 investigated the ignition and combustion of single biomass pellets in a vertical heating tube  
46 furnace, and identified two possible ignition behaviours: homogeneous ignition of volatile  
47 and heterogeneous ignition on the biomass particles' surface. More recently, Li et al. <sup>[3]</sup>  
48 conducted ignition tests of biomass particles by experimentally detecting the change of  
49 luminance inside of a down-fire reactor before and after biomass injection, and results

50 revealed that there is a significant effect of particle size on the ignition temperature and  
51 ignition delay time, and suggested that the ignition mechanism of biomass could be switched  
52 between homogeneous ignition and heterogeneous ignition. However, biomass feedstock is a  
53 highly diverse solid fuel and its chemical composition varies greatly from one source to  
54 another, same as their ignition behaviour. Therefore, it is highly essential to develop  
55 fundamental knowledge that could potentially be used to predict ignition characteristics of a  
56 wider range of biomass feedstock.

57 Due to the major organic substances of biomass can be divided into three main chemical  
58 components: cellulose, hemicellulose and lignin<sup>[9]</sup>, their distinct thermal characteristics have  
59 been often applied as an effective means to provide generalised understandings of various  
60 thermal processes of biomass, as well as identify their mutual interactions along thermal  
61 conversion processes<sup>[10-13]</sup>. Thermal conversion of biomass has been studied on the basis of  
62 these three main components in recent, as well as their interactions, since the mutual  
63 interactions can affect their thermal behaviour. Raveendran et al.<sup>[10]</sup> found no detectable  
64 interactions among the components during the thermal conversion process through the study  
65 of their thermal characteristics on the TGA and packed-bed pyrolyzer. Yang et al.<sup>[14]</sup> also  
66 observed negligible interactions among the three components in their studies by using a TGA  
67 analyzer, as well as in Wang et al<sup>[13]</sup> study. However, Worasuwannarak et al<sup>[11]</sup> observed  
68 significant interactions between the components by studying the yield of liquid productions,  
69 similar interactions are also reported by Wang et al.<sup>[12]</sup> and Stefanidis et al<sup>[15]</sup>. The ignition  
70 behaviour of biomass could also be affected by interactions among the major components  
71 during combustion process, such research however is rarely reported. Studying the  
72 performances of ignition behaviour of different component mixtures will allow a further  
73 identification of potential interactions among the major components, and also enables the  
74 prediction of the ignition behaviour of biomass feedstock.

75 Apart from the physical and chemical studies on the interactions, kinetic study on the  
76 interactions is rarely reported. Thermal conversion of biomass can be classified as  
77 heterogeneous chemical reaction, its reaction kinetics can be affected by its three key  
78 components<sup>[16, 17]</sup>. Through the reaction kinetic study, the difference between activation  
79 energy ( $E_a$ ), and pre-exponential factor ( $A$ ) can be obtained to better understand the  
80 interactions among the components.

81 In this paper, first, we will characterise the ignition behaviour of the three main chemical  
82 components of biomass. Then, ignition characteristics of various mixtures of these chemical  
83 components will be fully discussed to quantify the effects of interactions between the organic  
84 components on the overall ignition behaviour. Finally, the ignition properties of mixtures of  
85 these chemical components to simulate an artificial biomass will be conducted and compared  
86 with that of natural biomass of wheat straw and soft wood, as well as the calculation of  
87 kinetic parameters, with the aim of identifying the potential interactions among them with  
88 regards to ignition behaviour.

## 89 **2. Materials and methods**

### 90 *2.1 Materials and sample preparation*

91 Cellulose and Xylan (corn cob xylan) powder are purchased from Sigma-Aldrich, and lignin  
92 (dealkaline lignin) powder is purchased from Carbosynt. Xylan has been often considered as  
93 a representative molecule for hemicellulose<sup>[14]</sup>. The proximate and ultimate analysis of these  
94 samples as well as of the wheat straw and soft wood are presented in Table 1. As it can be  
95 observed from the analysis, the contents of volatile matter in cellulose and xylan is higher  
96 than in lignin, while lignin has a much higher fixed carbon and ash content. For  
97 lignocellulosic biomass, the largest component is cellulose with over 40% of its overall

98 weight, which will be majorly converted to gaseous and liquid products during its thermal  
 99 conversions; hemicellulose, the least stable component, accounts for approximately 30% by  
 100 weight of initial biomass; while lignin normally accounts for approximately 20% by weight,  
 101 40% of which attributes to char yield after pyrolysis <sup>[18-20]</sup>.

102 Table 1. Proximate and ultimate data of biomass samples (wt. %)

	Cellulose	Xylan	Lignin	Wheat Straw	Soft Wood
Moisture <sup>ar</sup>	2.70	2.90	3.20	2.30	3.50
VM <sup>db</sup>	89.70	84.80	51.30	74.80	58.36
Ash <sup>db</sup>	1.70	1.70	15.00	7.40	1.12
FC <sup>db</sup>	8.60	13.50	33.70	17.80	40.52
C <sup>db</sup>	42.18	38.41	62.09	45.20	58.28
H <sup>db</sup>	6.15	6.18	5.88	5.25	4.71
O <sup>db</sup>	51.66	55.40	30.52	48.84	36.51
N <sup>db</sup>	0.01	0.01	0.51	0.71	0.50

103 *db: dry basis; ar: as received*

## 104 2.2 Experiment design

105 Table 2. Summary of testing conditions

		Mixing ratio (%)	Heating rate (°C/min)	Final temp. (°C)
Individual samples	Cellulose	-	20	900
	Xylan	-	20	900
	Lignin	-	20	900
	Wheat straw	-	20	900
	Soft wood	-	20	900
Mixture samples	Cellulose / Xylan	50/50	20	900
	Cellulose / Lignin	50/50	20	900
	Xylan / Lignin	50/50	20	900
Artificial samples*	Wheat straw	Cellulose / Xylan / Lignin 61.3/19.3/19.4	20	900
	Soft wood	Cellulose / Xylan / Lignin 43.1/24.1/32.8	20	900

106 \* *The ratio is summarised from the literature [13, 21]*

107 The Coning and Quartering Method <sup>[22]</sup> is applied to prepare the mixture samples in this  
 108 study. This method has demonstrated its advantages for preparation of samples with poor  
 109 flowability, which can reduce the sampling size of the powder sample without generating a  
 110 systematic bias. Individual samples are mixed in a container according to the predetermined

111 mixing ratio in the experiment design, as detailed in Table 2, followed by the mixing  
112 procedures: 1) pour a cone of the mixture into a plate; 2) divide the cone into halves; 3)  
113 divide the cone into quarters; 4) discard the two opposite quarters of the sample; 5)  
114 recombine the remaining sample. The procedure is repeated three times to prepare each  
115 mixture sample. A total of 10 samples are prepared, as listed in Table 2.

### 116 *2.3 Estimation of the ignition temperature*

117 Ignition temperature is identified as the lowest temperature at which a solid fuel starts to  
118 ignite without the aid of an external ignition sources. In theory, ignition temperature is the  
119 temperature to which a fuel-air mixture must be increased so that the heat evolved by the  
120 exothermic reactions of the combustion system will just overbalance the rate at which heat is  
121 discharged to the surroundings <sup>[23]</sup>. Ignition temperature of solid fuels is often determined by  
122 empirical methods through thermogravimetric (TG) and differential thermogravimetric  
123 (DTG) curves, such as: (1) identify the temperature at which the mass loss curve in the  
124 combustion (oxidative atmosphere) diverges from that of pyrolysis (inert atmosphere) <sup>[24, 25]</sup>;  
125 (2) identify the temperature at which it starts the maximum reactivity of devolatilization <sup>[26]</sup>.  
126 Considering the replicability and reliability of the results <sup>[27]</sup>, method (1) will be employed in  
127 this study to determine the ignition temperature in this work. This method is based on the  
128 principle that when the fuel sample is ignited, two exothermic peaks appear before and after  
129 the turning point at where the TG curves of combustion and pyrolysis are diverged <sup>[28]</sup>.  
130 However, there might exist crosses of TG curves of combustion and pyrolysis when the  
131 diverging point is undistinguishable; if this turns out to be the case, DTG curves will be used  
132 as a complementary information, and the diverging point will be defined as where the second  
133 peak of the combustion curve appears.

### 134 *2.4 Determination of kinetics*

135 The kinetics of biomass thermal conversions can be expressed by following equation:

$$136 \quad \frac{d\alpha}{dt} = k(T)f(\alpha) = A \exp\left(\frac{-E_a}{RT}\right) f(\alpha) \quad (\text{Eq.1})$$

137 where  $T$  is the absolute temperature;  $R$  is the gas constant;  $f(\alpha)$  is the mass conversion  
138 function;  $\alpha$  is the conversion fraction, which represents the relationship between the initial  
139 mass ( $m_0$ ) and the final mass ( $m_\infty$ ), and the current mass ( $m$ ) of the sample, as given below:

$$140 \quad \alpha = \frac{m_0 - m}{m_0 - m_\infty} \quad (\text{Eq.2})$$

141 When the heating rate ( $\beta = dT/dt$ ) is constant, Eq. 1 can be integrated as:

$$142 \quad g(\alpha) = \int_0^\alpha \frac{d\alpha}{f(\alpha)} = \frac{A}{\beta} \int_0^T dT \exp\left(-\frac{E_a}{RT}\right) \quad (\text{Eq.3})$$

143 where  $g(\alpha)$  is an integrate function, consequently, Eq.3 can be approximated by:

$$144 \quad \ln\left[\frac{g(\alpha)}{T^2}\right] = \ln\left[\frac{AR}{\beta E_a}\left(1 - \frac{2RT}{E_a}\right)\right] - \frac{E_a}{RT} \quad (\text{Eq.4})$$

145 The conversion function  $f(\alpha)$  depends on the operating conditions and the stage of the  
146 combustion. Combustion is a complicated process, which normally can divided into three  
147 different reaction stages <sup>[29]</sup>, or two parallel reactions with three reaction stages <sup>[30]</sup>, or more  
148 recently two-stage reactions with the first step that occurs at lower temperature and the  
149 second step that occurs the oxidation of char at higher temperature <sup>[31]</sup>. Thermal  
150 decomposition of biomass has been commonly described as first-order reaction <sup>[32]</sup>. In this  
151 study, we consider the combustion process with two-stage reaction mechanism, and both  
152 stages are governed by the first order reaction law. In this case,  $f(\alpha) = (1 - \alpha)$ , as a result,  $g$   
153 ( $\alpha$ ) =  $-\ln(1 - \alpha)$ , and for most system  $RT/E_a \ll 1$  <sup>[33]</sup>, then Eq.4 can be approximated by:

$$154 \quad \ln\left[\frac{-\ln(1-\alpha)}{T^2}\right] \approx \ln\left(\frac{AR}{\beta E_a}\right) - \frac{E_a}{RT} \quad (\text{Eq.5})$$

155 The left hand side of Eq.5 is plotted against  $1/T$  for the data from a single heating rate, which  
156 leads to a straight line, from which the activation energy can be obtained as the slope of this  
157 line, and the pre-exponential factor is derived from its intercept.

### 158 3. Results and discussion

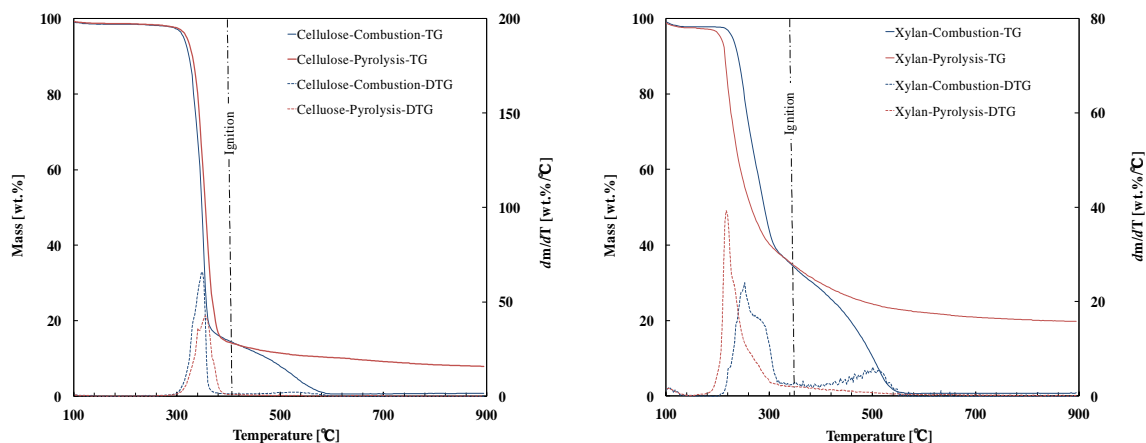
#### 159 3.1 Thermal characteristics of cellulose, xylan and lignin and their ignition temperatures

160 Fig. 1 (a-c) show the mass loss profiles of cellulose, xylan and lignin in air and nitrogen  
161 atmospheres at a heating rate of 20°C/min up to a final temperature of 900°C. Due to the  
162 different chemical structures of the individual components, substantial differences in the  
163 thermal characteristics among them could be expected<sup>[34]</sup>.

164 Fig.1 (a) shows that cellulose starts to decompose at a temperature of 325°C and losses over  
165 80% of its mass before 410°C, which is close to the content of its volatile matter as shown in  
166 Table 1. When temperature is greater than 410°C, the mass loss curves along its pyrolysis and  
167 combustion processes start to diverge, where the pyrolysis curve tends to flatten without  
168 further decomposition, and the solid residues account for approximately 8% of its initial mass  
169 at the end of the process; while the combustion curve shows that a continuous mass loss  
170 occurred until 600°C with less than 1% inert residues left in the end. The difference between  
171 the amounts of solid residue after pyrolysis and combustion processes equals to the content of  
172 the fixed carbon in cellulose. Fig.1 (b) shows that the decomposition of xylan starts at the  
173 temperature of 190°C and the divergence of its pyrolysis and combustion curves occurs at  
174 370°C, where the pyrolysis rate is getting stable while a second drop of mass occurs in  
175 combustion process due to char oxidation. The solid residue left after pyrolysis and  
176 combustion processes are 18% and 1.5% of the initial mass of xylan respectively.

177 In Fig.1 (c), the show shows that the decomposition of lignin starts at 210°C and the curves of  
178 pyrolysis and combustion diverged at 405°C. A slow decomposition of lignin is noticed at the  
179 temperature ranges from 405°C to 750°C in its pyrolysis, and the remaining accounts for  
180 approximately 45% of its initial mass after pyrolysis; while in combustion, lignin loses more  
181 than half of its mass at the temperature ranges from 405°C to 600°C, and there is 15% of its

182 mass left in the end, which equals to its ash content.

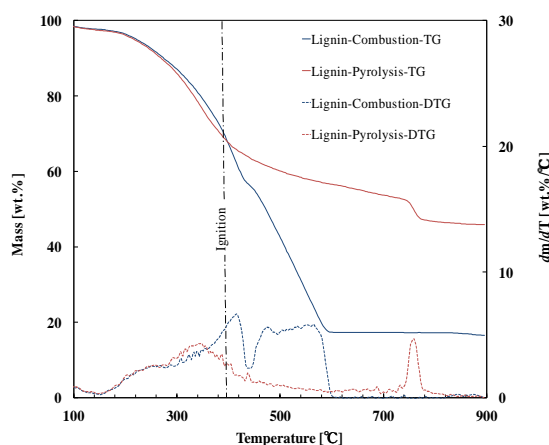


183

184

(a) Cellulose

(b) Xylan



185

186

(c) Lignin

187 Fig.1. Thermal characteristics of individual chemical components in air (combustion) and nitrogen (pyrolysis)

188

with identified ignition temperatures

189

By comparing TGA profiles of cellulose, xylan, and lignin in Fig.1, nearly all of their mass

190

loss curves of pyrolysis and combustion processes coincide on top of the each other before

191

the divergence occurred, a slight deviation might be caused by the difference of thermal

192

conductivity of nitrogen and air<sup>[3]</sup>. This implies that, at the early stage of thermal conversion,

193

temperature is the dominant factor of the reactions, rather than the existence of oxygen.

194

Among these three samples, cellulose has the narrowest decomposition temperature range

195 and lost the most of its mass during the decomposition process, while lignin has the widest  
 196 decomposition temperature range and generates the most residual. The ignition temperatures  
 197 of cellulose, xylan, and lignin are 410°C, 370°C, and 405°C respectively. These temperatures  
 198 are identified as the diverging point of TG curves and are the same temperatures at which the  
 199 second peak appears in the DTG curves under air conditions.

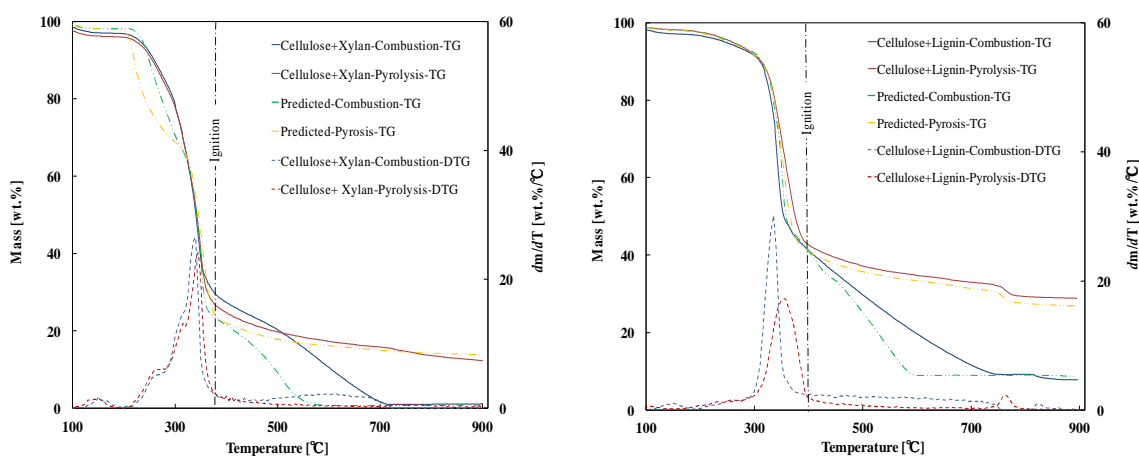
### 200 3.2 Ignition characteristics of mixtures of xylan, cellulose, and lignin

201 The thermal behaviour (mass loss) of the mixtures could be predicted using the weighted sum  
 202 of the partial contributions of individual components <sup>[10]</sup> as described by the following  
 203 equation:

$$204 \quad \frac{dm_{mix}}{dt} = \sum_i y_i \frac{dm_i}{dt} \quad (\text{Eq.6})$$

205 where  $y_i$  refers to the mass fraction of component  $i$  in the mixture. So that the TG and DTG  
 206 curves could be drawn based on the calculation results, and then the ignition temperatures of  
 207 these mixtures would be predictable. To quantify the interactions of individual components  
 208 on the ignition temperature of mixtures, the thermal tests of various mixtures of chemical  
 209 components in air and nitrogen are performed and the results along with the predicted thermal  
 210 characteristics of the mixtures are shown in Fig.2 (a-c). The potential impacts of interactions  
 211 on the determined ignition temperatures will be discussed in this section.

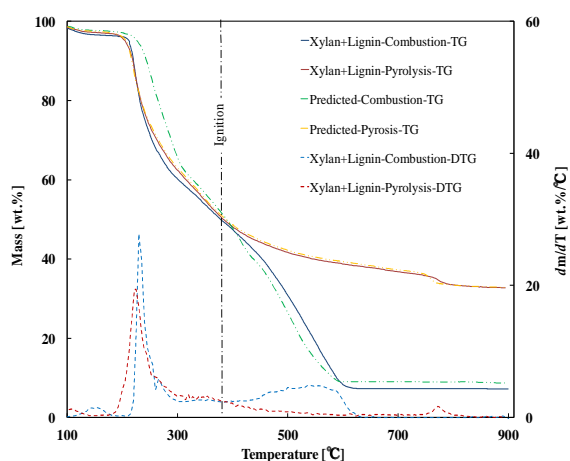
212



213

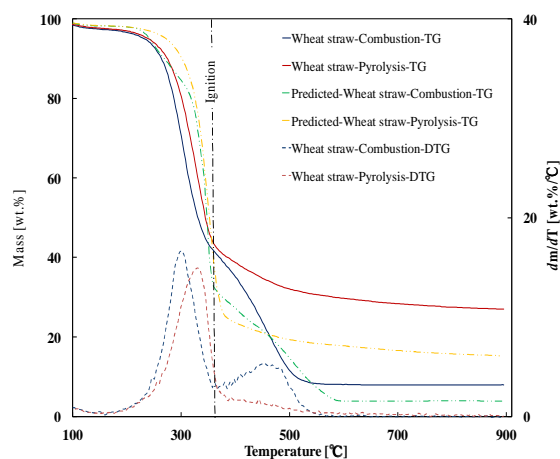
214

(a) Mixture of Cellulose and Xylan



215

(b) Mixture of Cellulose and Lignin



216 (c) Mixture of Xylan and Lignin

217 (d) Mixture of Cellulose, Xylan and Lignin (as a  
218 prediction of wheat straw)

218 Fig 2. Thermal characteristics of mixtures of components in air (combustion) and nitrogen (pyrolysis) with  
219 identified ignition temperatures along with the prediction results

220 Fig.2 (a) shows the experimental and predicted results of the mixture of cellulose and xylan,  
221 its decomposition starts at a temperature of 250°C, same as the predicted starting temperature.  
222 The significant release of volatile matter of the mixture occurred at the temperature range of  
223 250°C to 350°C, nearly the same as the predicted temperature range. Although there is an  
224 obvious burnout delay in the experimental combustion curve compared to that from  
225 prediction, where the sample in the experimental curve keeps decomposing till reaching  
226 700°C, which is a much higher temperature than the ending decomposition temperature of the  
227 predicted curve, that is 550°C, however, this does not affect the identification of ignition  
228 temperature. The decomposition of xylan particles at lower temperatures could potentially  
229 form a charred film that, acted as a barrier, warps nearby cellulose particles, so that the mass  
230 and heat transfer of and between the particles is limited, as stated in Stylianos et al. <sup>[15]</sup> and  
231 Wang et al. <sup>[13]</sup> studies. There are two detectable diverging temperatures observed in the TG  
232 curves of the mixture of cellulose and xylan: one is 370°C, and the other is 510°C, leading to a

233 difficult identification of ignition temperature. To address this, the DTG curves are used as  
234 complementary information, and the ignition temperature of the mixture is defined at 405°C,  
235 compared with the predicted one at 400°C, indicating that the ignition temperature of the  
236 mixture can be predicted from the sum of the individual decomposition data of the mixture  
237 component.

238 Fig.2 (b) shows the decomposition performance of the mixture of cellulose and lignin, which  
239 agrees well with the predicted decomposition behaviour. When the temperature reaches to  
240 400°C, the pyrolysis and combustion curves start to diverge, however, there is an obvious  
241 difference in the combustion curve between the experimental and the predicted at the  
242 temperature range of 420-730°C. A prolonged combustion is observed in the experimental  
243 curve, this might be caused by the melting and forming of agglomeration of lignin particles,  
244 and the agglomerated lignin wrapping nearby cellulose particles <sup>[15]</sup>, lowering the heat  
245 transfer efficiency of the particles. In addition, the structure of lignin consists of  
246 phenylpropane coupled with C-C bond and/or C-O-C bond, which covers an extremely wide  
247 decomposition temperature range (152-700°C) <sup>[15]</sup>. Accordingly, above reasons may lead to a  
248 higher temperature to burnout, while the ignition characteristics are not affected. The  
249 diverging point of the curves in the experiment data occurs at 400°C from both TG and DTG  
250 results, meaning that the ignition temperature of the mixture is 400°C, the same as the  
251 prediction.

252 Fig.2 (c) shows the experimental and predicted thermal performance of the mixture of xylan  
253 and lignin, which starts to decompose at 210°C. When temperature exceeds 400°C, the  
254 pyrolysis curve becomes flat, while the combustion curve continues to drop till 600°C. Both  
255 experimental curves coincide with the predicted ones. The diverging point of the curves in  
256 the test occurs at 400°C, which can also be identified in the DTG curves, indicating the

257 ignition temperature of the mixture of xylan and lignin is 400°C.

258 At last, a comparison of experimental and predicted performance of wheat straw is presented  
259 in Fig.2 (d). The predicted results are similar to that of wheat straw, the decomposition starts  
260 at 230°C. When the temperature reaches 350°C, pyrolysis curves become flat according to  
261 both experimental and predicted results. The combustion curves, however, start the second  
262 drop, which is known as char oxidation stage. Since compositions in the wheat straw is more  
263 complicate than that in pure component of cellulose, xylan or lignin; this leads to a higher  
264 amount of remaining solids from the experiment results when compared with the predicted  
265 result, both in pyrolysis and combustion tests. The departing point of the curves in the  
266 experiment is at 350°C, a same result was obtained from the DTG curve; while there are two  
267 diverging points observed in predicted curves, the first point agrees well with the  
268 experimental result, indicating the ignition temperature of wheat straw could also be acquired  
269 by predictions.

270 As discussed above, the determined ignition temperatures of mixtures (cellulose and lignin,  
271 xylan and lignin) are close to the ignition temperature of lignin. Cellulose and xylan have a  
272 higher volatile matter content, which means that the major part of them have been released at  
273 the pyrolysis stage; lignin, however, has the highest fixed carbon content of all of them,  
274 which contributes to the significant amount of char yield after pyrolysis. According to Kai et  
275 al. <sup>[34]</sup>, at the combustion stage, the oxidation of the formation of char is characterised by the  
276 existence of lignin. This might result in the ignition temperatures of lignin mixtures, being  
277 close to the ignition temperature of lignin itself. From the experimental data of all the  
278 mixtures, it is observed that the pyrolysis results could be predicted with precision, similar  
279 conclusions were also reported by Stylianos et al <sup>[15]</sup>. The synergistic effects between  
280 components are less significant but can be observed through the study of combustion curves.

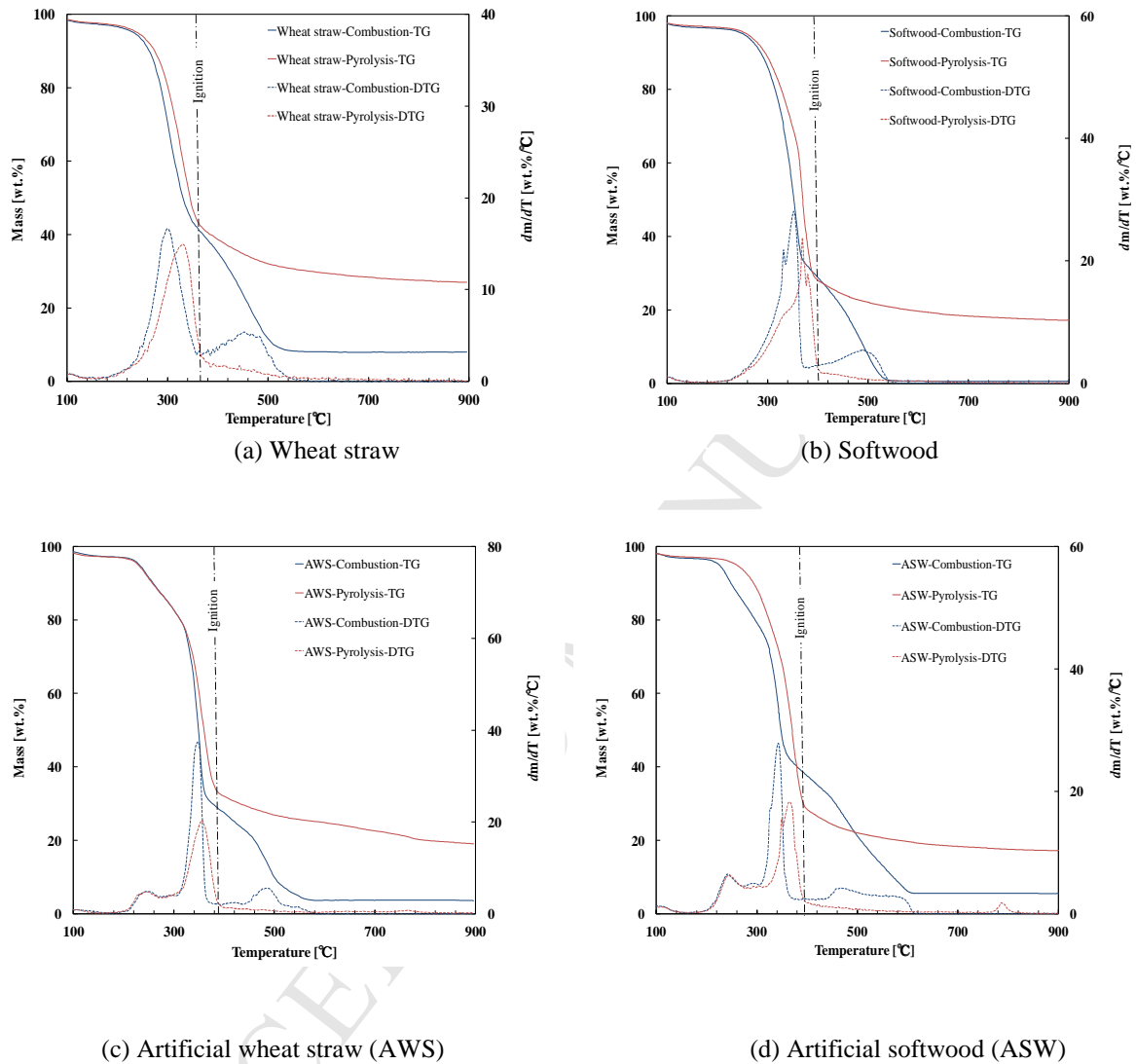
281 There is no significant influence on the ignition behaviour when physically mixing cellulose,  
282 xylan and lignin.

### 283 *3.3 Thermal characteristics and ignition temperatures of natural and artificial biomass*

284 To further identify the interaction of chemical components on the ignition properties of  
285 biomass, natural and artificial samples (artificial wheat straw (AWS) and artificial soft wood  
286 (ASW)) are tested. The mass fraction of cellulose / hemicellulose / lignin in AWS and ASW  
287 that we assumed are 61.3/19.3/19.4 and 43.1/24.1/32.8 respectively. Thermal characteristics  
288 of the samples of pyrolysis and combustion are examined by using TGA at the heating rate of  
289 20°C/min, the results are presented in Fig. 3.

290 The decomposition of wheat straw starts at 250°C and softwood starts at 255°C, and wheat  
291 straw lost 60% of its mass when temperature reaches 350°C, while softwood lost nearly 70%  
292 of its mass when temperature reaches 405°C, the mass loss is caused by the release of  
293 moisture and volatile content in the mixture, after these temperature points, the pyrolysis and  
294 combustion curves start to diverge. When temperature exceeds the diverge points, the  
295 pyrolysis curve keeps flattering out till ending, and there is 25% of its initial mass left as solid  
296 residue for wheat straw while it is 20% for softwood, the residue consists of fixed carbon and  
297 ash; however, the combustion curve shows a second mass drop, and wheat straw ends at  
298 520°C, while softwood finishes at 510°C, leading to a further mass loss ending with an 18%  
299 and 39% of its initial mass of wheat straw and softwood respectively, corresponding to the  
300 fixed carbon content. In DTG curves, two obvious peaks appear before diverge temperature  
301 for both samples, the first one at 100°C, caused by the evaporation of moisture, and as for the  
302 second one, it is 300°C for wheat straw and 330°C for soft wood, due to the release of the  
303 volatile matter. Then pyrolysis curve becomes stable, while combustion curve shows a third  
304 peak at 460°C for wheat straw, and 500°C for soft wood, due to the oxidation of char. In

305 consequence, the ignition temperature of wheat straw and softwood is 350°C and 405°C  
 306 respectively, which can also be observed from the DTG curve in Fig. 3 (a) and (b), similar  
 307 ignition temperatures can also be obtained from the studies of [3, 35],



308

309

310 Fig.3. Thermal characteristics of biomass samples in air and nitrogen with identified ignition temperature:

311 (a) wheat straw; (b) soft wood; (c) artificial wheat straw (AWS); (d) artificial softwood (ASW)

312 Fig. 3 (c) and (d) show the thermal decomposition results for artificial biomass with the  
 313 similar trends as that of natural biomass. The first phase decomposition of artificial wheat  
 314 straw (AWS) starts at 220°C and ends at 365°C, two step decreasing of mass occurred during  
 315 this phase, both in pyrolysis and combustion curves. The first decrease starts from 220°C to

316 340°C in TG curves, reaching its peak at 260°C in DTG curves, this is mainly caused by the  
317 decomposition of xylan, the least thermally stable component in biomass <sup>[36]</sup>, due to the  
318 breakdown of its C-O-C and some pyranose C-C bonds <sup>[37]</sup>. According to the individual  
319 component tests, xylan starts to decompose at 180°C and sharply loses 65% of its mass before  
320 300°C, while partial cellulose and lignin start to decompose at lower temperatures, this  
321 implies that the existence of cellulose and lignin doesn't affect the thermal behaviour of xylan  
322 significantly. The second decrease starts from 340°C to 380°C in the TG curves, and as can be  
323 seen in the DTG curve, it reaches its peak at 355°C. As illustrated in Fig. 1, during this  
324 temperature range, cellulose loses nearly 90% of its initial mass, lignin loses 15%, and xylan  
325 loses only 4%, indicating that cellulose and lignin are the main components that attribute the  
326 mass loss during this stage. The pyrolysis and combustion curves of AWS start to diverge at  
327 375°C. After that, in the pyrolysis scenario, AWS continues to lose mass very slowly with a  
328 remaining of 20% of its initial mass at the end of the test, which is the same as the sum of  
329 partial contributions of fixed carbon and ash contents of each component. While for the  
330 combustion scenario, most of the mass loss at the char oxidation stage is attributed to lignin  
331 and xylan, since both of them have higher fixed carbon contents (33.7 wt.% in lignin; 13.5  
332 wt.% in xylan) compared to cellulose (8.6 wt.%). As shown in both TG and DTG curves, the  
333 ignition temperature of the AWS is 375°C.

334 As for artificial softwood (ASW), similar conclusion can be summarised as AWS, the  
335 decomposition of each component is distinguishable. The first phase decomposition begins at  
336 210°C, till to 360°C for combustion and it is 240°C-390°C for pyrolysis, two drops of mass  
337 occurred during this phase. The first drop starts from 210°C to 330°C in combustion curve,  
338 while it is 240°C-350°C for pyrolysis curve. As showed in Table 2, the content of xylan in  
339 ASW is similar to that of AWS, which leading to the semblable temperature range of first  
340 drop. The second drop of mass happened from 330°C to 360°C in combustion curve and from

341 350°C to 390°C in pyrolysis curve, due to the decomposition of cellulose and lignin. After  
342 390°C, the pyrolysis curve becomes flat and with 20% remaining at the end; while the  
343 combustion curve happened the char oxidation phase, and the remaining equals to the sum of  
344 partial contributions of ash contents of each component. There are two notable diverging  
345 points in Fig 3 (d), one is 385°C, and the other one is 495°C, by complementing the DTG  
346 information, the ignition temperature of ASW is defined at 395°C, similar to that of natural  
347 softwood. It can be seen that the ignition temperature of ASW is close to that of lignin, since  
348 the fraction of lignin in ASW is much higher than that in AWS, indicating that the lignin is  
349 the dominant factor that influence the ignition temperature of the samples.

350 As discussed above, thermal behaviour of AWS and ASW could be predicted through the  
351 sum of the decomposition behaviour of individual components. As aforementioned, the  
352 ignition temperature and thermal behaviour of the artificial biomass is similar to that of  
353 natural biomass, meaning that the ignition temperatures of various biomass materials are  
354 predictable once the mass fractions of these individual components are certain. Nevertheless,  
355 there is a slight difference between the ignition temperature of natural and artificial biomass  
356 can be observed, reveals the potential interactions among the three chemical components in  
357 natural biomass, which might affect its ignition behaviour; also, the moisture content of the  
358 artificial biomass is different from that of natural biomass, and the variation of moisture  
359 content in the samples may have an influence on the ignition characteristics<sup>[38]</sup>, a summary of  
360 the comparison of moisture content and ignition temperature is list below in Table 3. It can be  
361 seen that the higher the moisture content, the higher the ignition temperature. The increased  
362 moisture content will increase the thermal properties of materials, like: thermal conductivity  
363 and specific heat, as well as the vaporization and migration of moisture<sup>[39]</sup>, leading to the  
364 delay of ignition as a function of external heat flux and substantially alters the thermos-  
365 physical properties of the biomass samples<sup>[40]</sup>.

366 It also should be noticed that the structures of cellulose, xylan and lignin in biomass differ  
 367 from the commercial materials, as well as in the different biomass fuels, and the different  
 368 structures would result in varying ignition properties. Besides, the structure of biomass is  
 369 complicated, the chemical component cellulose provides the skeletal structure of the biomass  
 370 that is coated with hemicellulose and cemented by lignin <sup>[20, 41]</sup>, co-existence with the ash and  
 371 moisture; the artificial biomass is made by physical mixing of these three components that is  
 372 unable to mimic the inner tangles of them precisely. Above results can provide a general  
 373 perspective of the ignition behaviour of three chemical components and their mixtures, and to  
 374 predict the ignition temperature of natural biomass.

375 Table 3. The summary of moisture content and ignition temperature of natural and artificial biomass.

	Wheat straw	Artificial wheat straw	Softwood	Artificial softwood
Moisture content (wt. %)	2.30	2.84*	3.50	2.91*
Ignition temperature (°C)	350	375	405	395

376 *\*The moisture content of artificial biomass is the sum of partial contributions of moisture content of each*  
 377 *component.*

### 378 3.3 Kinetic study on the interactions

379 Former study on the ignition behaviour of samples has indicated the possibilities to estimate  
 380 the ignition temperature of biomass when the fractions of three chemical components are  
 381 certain, but the variation of the ignition temperatures between artificial and natural biomass  
 382 illustrates the potential interactions among the chemical components may influence the  
 383 ignition behaviour. In order to further understand the mutual interactions, and how they affect  
 384 the combustion process, Coats-Redfern method was used to calculate the kinetic parameters  
 385 of the combustion of all the samples, and the changes of activation energy ( $E_a$ ) and pre-  
 386 exponential factor ( $A$ ) will be discussed to investigate the interactions among the cellulose,  
 387 xylan and lignin.

388 As discussed in *Sec. 2.4*, the process of combustion in this study is divided into two steps:  
389 pyrolysis and char oxidation. The combustion kinetic parameters of the studied individual  
390 components and the one from the mixture samples obtained from the calculations are shown  
391 in Table 4, together with the summarised ignition temperatures. At the stage of pyrolysis, the  
392 values of  $E_a$  for cellulose, xylan and lignin are 223.32 kJ/mol, 73.85 kJ/mol and 23.41 kJ/mol  
393 respectively. Cellulose has the highest  $E_a$  value among them, followed by xylan, similar  
394 results are also reported by Milosavljevic et al. <sup>[42]</sup>. This result indicates that the  
395 decomposition of cellulose is a crucial step to determine the overall rate of the biomass  
396 combustion process <sup>[17]</sup>, while xylan and lignin dominate the initial decomposition.

397 The obtained correlation coefficients ( $R^2$ ) of cellulose and xylan at their second step are not  
398 high enough to be trusted, indicating a completion of decomposition of cellulose and xylan at  
399 the early stage of pyrolysis, so that the first order reaction model might not be suitable for the  
400 combustion of cellulose and xylan <sup>[43]</sup>. While the correlation coefficient at the step 2 of  
401 combustion of lignin is reliable, indicating the feasibility of first order reaction model on both  
402 steps of combustion of lignin. The  $E_a$  value for lignin in step 2 is 45.98kJ/mol, higher than  
403 that of step 1, this is attributed to the high energy required to decompose inorganic matter <sup>[44]</sup>,  
404 since lignin has the highest ash content among these three components.

405 For the mixture of cellulose and xylan, the  $E_a$  value in step 1 is 54.64 kJ/mol which is lower  
406 than that of either cellulose or xylan, suggests the potential interactions between them could  
407 affect the reaction process during the pyrolysis. At devolatilization stage, xylan begins to  
408 decompose prior to cellulose and forming char residues that might cover and wrap around the  
409 cellulose surface, which inhibits the release of volatile products and enhances the secondary  
410 degradation of macromolecular materials in cellulose. For the mixture of cellulose and lignin,  
411  $E_a$  value is 152.74 kJ/mol in step 1, which is placed in between of that of cellulose and xylan.  
412 The existence of lignin in the mixture enhances the cellulose to generate small molecular

413 products during the devolatilization process <sup>[45]</sup>, so that the mixture requires lower energy to  
 414 devolatilize compared to cellulose. And the  $E_a$  value for the mixture of lignin and xylan is  
 415 62.01 kJ /mol in step 1, which is in the range of the activation energy of lignin and xylan.  
 416 However, for all the three mixtures, correlation coefficients are all rather small in their  
 417 second step, indicating the first order reaction model is not suitable for describing the  
 418 combustion of mixtures.

419 Table 4. Kinetic parameters of combustion of individual component.

	Ignition temp. (°C)	Temp. range ( °C)	$E_a$ (kJ/mol)	A (1/s)	$R^2$
Cellulose	410	314-362 <sup>①</sup>	223.32	5.87E+18	0.9967
		382-584 <sup>②</sup>	-	-	-
Xylan	350	230-308 <sup>①</sup>	73.85	2.76E+06	0.9385
		310-550 <sup>②</sup>	-	-	-
Lignin	405	223-453 <sup>①</sup>	23.41	4.03E+00	0.9934
		456-591 <sup>②</sup>	45.98	2.88E+02	0.9329
Cellulose & Xylan	405	245-355 <sup>①</sup>	54.64	1.01E+04	0.9824
		400-700 <sup>②</sup>	-	-	-
Cellulose & Lignin	400	320-350 <sup>①</sup>	152.74	4.27E+12	0.9892
		360-710 <sup>②</sup>	-	-	-
Lignin & Xylan	400	212-269 <sup>①</sup>	62.01	2.89E+05	0.8437
		277-595 <sup>②</sup>	-	-	-
Wheat straw	350	247-352 <sup>①</sup>	62.58	2.69E+05	0.9814
		352-502 <sup>②</sup>	20.31	5.19E+00	0.9746
AWS	375	248-358 <sup>①</sup>	44.93	9.41E+02	0.8753
		361-551 <sup>②</sup>	17.43	2.86E+00	0.7952
Soft wood	405	260-380 <sup>①</sup>	70.46	2.22E+05	0.9889
		390-510 <sup>②</sup>	23.83	9.76E+00	0.9016
ASW	395	227-363 <sup>①</sup>	40.67	4.25E+02	0.9557
		377-570 <sup>②</sup>	13.45	8.14E-01	0.8891

420 Note: <sup>①</sup>step 1 (pyrolysis) of the combustion process; <sup>②</sup>step 2 (char oxidation) of the combustion process

421 The obtained kinetic parameters of the natural and artificial biomass are also listed in Table 4.  
 422 In step 1, the value of  $E_a$  for the natural biomass are all higher than that of the artificial  
 423 biomass, with 62.85 kJ/mol and 70.46 kJ/mol for wheat straw and softwood respectively,

424 compared to 44.93 kJ/mol and 40.67 kJ/mol for artificial wheat straw and artificial softwood  
425 respectively. Same trends are also observed by the results of step 2, the value of  $E_a$  for the  
426 natural biomass are within 20-25 kJ/mol, while it is 13-18 kJ/mol for the artificial biomass. It  
427 can be seen, the activation energy obtained in step 2 are all smaller than that in step 1,  
428 meaning that the char oxidation requires less energy to react than the release of volatile  
429 matter. Meanwhile, the values of  $E_a$  for artificial biomass are all smaller than that of natural  
430 biomass in both two steps. In fact, there exist interactions among cellulose, hemicellulose and  
431 lignin in natural biomass, such as the existence of hydrogen bonding between cellulose and  
432 lignin<sup>[46]</sup>, as well as cellulose and hemicellulose, and also the presence of covalent linkages  
433 between cellulose and lignin<sup>[47]</sup>, these bonds require more energy to break up, leading to the  
434 higher value of  $E_a$  for natural biomass than that of artificial biomass. Besides, the chemical  
435 and physical interactions within cellulose-hemicellulose-lignin in actual biomass could  
436 generate different local reaction conditions<sup>[46]</sup> which cannot be mimicked in a simple  
437 physical mixture of the individual components. All these could result in the difference of  
438 kinetic results between natural and artificial biomass.

439 For the tests of mixtures and biomass, the calculated  $E_a$  are within the approximate range  
440 from 1 to 180 kJ/mol<sup>[48]</sup>. The obtained kinetic parameters reflect the fact that even when the  
441 components are physically mixed, the interactions among them affects the reaction process.

#### 442 **4. Conclusion**

443 In this paper, thermal behaviour of cellulose, xylan, lignin, their mixtures and natural biomass  
444 have been studied by using TGA. For all the tested samples, temperature is the dominant  
445 factor that influences their thermal behaviour at the pyrolysis stage, regardless of the presence  
446 of oxygen. Ignition temperatures of cellulose, xylan and lignin were determined by using TG  
447 and DTG curves as 410°C, 370°C and 405°C respectively. Thermal behaviour of the mixtures

448 could be predicted according to that of individual components, and the ignition temperature is  
449 dominated by lignin when lignin exists in the mixtures, while cellulose dominates the ignition  
450 temperature of the mixture of cellulose and xylan. The ignition temperature of natural wheat  
451 straw is 350°C when compared with 365°C of artificial wheat straw, and it is 405°C for natural  
452 softwood and 395°C for artificial softwood respectively, the influence of mutual interactions  
453 among the components on the ignition behaviour is insignificant, and the results  
454 demonstrated a similar thermal behaviour between native and artificial biomass. The reaction  
455 kinetics of the samples are studied by using Coats-Redfern method, and the results indicate  
456 that first order kinetic model was fitted to most of the samples in the tests, especially natural  
457 biomass. The study of the changing of activation energy values from the individuals to the  
458 mixtures revealed the influence of mutual interactions among the components is significant  
459 on the thermal conversion process during the combustion. Future efforts should focus on  
460 testing the different kinds of chemical components, monitoring the products yields/evolution  
461 and the structure changes of mixtures.

#### 462 **Acknowledgements**

463 Authors would like to thank the Scottish Funding Council-Global Challenge Research Fund  
464 and the EU-Biofuels Research Infrastructure for Sharing Knowledge (BRISK) for their  
465 financial support of this work.

#### 466 **References**

- 467 1. Zhao, H.-b., et al., Study on the Transformation of Inherent Potassium during the Fast-Pyrolysis Process of  
468 Rice Straw. *Energy & Fuels*, 2015. **29**(10): p. 6404-6411.
- 469 2. Nussbaumer, T., Combustion and co-combustion of biomass: fundamentals, technologies, and primary  
470 measures for emission reduction. *Energy & fuels*, 2003. **17**(6): p. 1510-1521.
- 471 3. Li, J., M.C. Paul, and K.M. Czajka, Studies of Ignition Behavior of Biomass Particles in a Down-Fire  
472 Reactor for Improving Co-firing Performance. *Energy & Fuels*, 2016. **30**(7): p. 5870-5877.
- 473 4. Grotkjær, T., et al., An experimental study of biomass ignition☆. *Fuel*, 2003. **82**(7): p. 825-833.

- 474 5. Yang, H., et al., Coal ignition characteristics in CFB boiler. *Fuel*, 2005. **84**(14): p. 1849-1853.
- 475 6. Jones, J., et al., Low temperature ignition of biomass. *Fuel Processing Technology*, 2015. **134**: p. 372-377.
- 476 7. Riaza, J., et al., Ignition behavior of coal and biomass blends under oxy-firing conditions with steam  
477 additions. *Greenhouse Gases: Science and Technology*, 2013. **3**(5): p. 397-414.
- 478 8. Shan, F., et al., An experimental study of ignition and combustion of single biomass pellets in air and oxy-  
479 fuel. *Fuel*, 2017. **188**: p. 277-284.
- 480 9. Zhang, L., C.C. Xu, and P. Champagne, Overview of recent advances in thermo-chemical conversion of  
481 biomass. *Energy Conversion and Management*, 2010. **51**(5): p. 969-982.
- 482 10. Raveendran, K., A. Ganesh, and K.C. Khilar, Pyrolysis characteristics of biomass and biomass components.  
483 *Fuel*, 1996. **75**(8): p. 987-998.
- 484 11. Worasuwannarak, N., T. Sonobe, and W. Tanthapanichakoon, Pyrolysis behaviors of rice straw, rice husk,  
485 and corncob by TG-MS technique. *Journal of Analytical and Applied Pyrolysis*, 2007. **78**(2): p. 265-271.
- 486 12. Wang, G., et al., TG study on pyrolysis of biomass and its three components under syngas. *Fuel*, 2008.  
487 **87**(4): p. 552-558.
- 488 13. Wang, S., et al., Influence of the interaction of components on the pyrolysis behavior of biomass. *Journal of*  
489 *Analytical and Applied Pyrolysis*, 2011. **91**(1): p. 183-189.
- 490 14. Yang, H., et al., In-depth investigation of biomass pyrolysis based on three major components:  
491 hemicellulose, cellulose and lignin. *Energy & Fuels*, 2006. **20**(1): p. 388-393.
- 492 15. Stefanidis, S.D., et al., A study of lignocellulosic biomass pyrolysis via the pyrolysis of cellulose,  
493 hemicellulose and lignin. *Journal of Analytical and Applied Pyrolysis*, 2014. **105**: p. 143-150.
- 494 16. Galwey, A.K. and M.E. Brown, Kinetic background to thermal analysis and calorimetry, in *Handbook of*  
495 *thermal analysis and calorimetry*. 1998, Elsevier. p. 147-224.
- 496 17. White, J.E., W.J. Catallo, and B.L. Legendre, Biomass pyrolysis kinetics: a comparative critical review with  
497 relevant agricultural residue case studies. *Journal of Analytical and Applied Pyrolysis*, 2011. **91**(1): p. 1-33.
- 498 18. Mohan, D., C.U. Pittman, and P.H. Steele, Pyrolysis of wood/biomass for bio-oil: a critical review. *Energy*  
499 *& fuels*, 2006. **20**(3): p. 848-889.
- 500 19. Diebold, J. and A. Bridgwater, Overview of fast pyrolysis of biomass for the production of liquid fuels, in  
501 *Developments in thermochemical biomass conversion*. 1997, Springer. p. 5-23.
- 502 20. Klass, D.L., *Biomass for renewable energy, fuels, and chemicals*. 1998: Academic press.
- 503 21. Di Blasi, C., et al., Product distribution from pyrolysis of wood and agricultural residues. *Industrial &*  
504 *Engineering Chemistry Research*, 1999. **38**(6): p. 2216-2224.
- 505 22. Campos-M, M. and R. Campos-C, Applications of quartering method in soils and foods. Vol. 7. 2017. 35-39.
- 506 23. Tetteh, J., E. Metcalfe, and S.L. Howells, Optimisation of radial basis and backpropagation neural networks  
507 for modelling auto-ignition temperature by quantitative-structure property relationships. *Chemometrics and*  
508 *intelligent laboratory systems*, 1996. **32**(2): p. 177-191.

- 509 24. Wang, C.a., et al., Pyrolysis and combustion characteristics of coals in oxyfuel combustion. *Applied Energy*,  
510 2012. **97**: p. 264-273.
- 511 25. Arenillas, A., et al., A TG/DTA study on the effect of coal blending on ignition behaviour. *Journal of*  
512 *Thermal Analysis and Calorimetry*, 2004. **76**(2): p. 603-614.
- 513 26. Wang, C., et al., Thermogravimetric studies of the behavior of wheat straw with added coal during  
514 combustion. *Biomass and Bioenergy*, 2009. **33**(1): p. 50-56.
- 515 27. Fan, Y.-s., et al., Ignition characteristics of pulverized coal under high oxygen concentrations. *Energy &*  
516 *Fuels*, 2008. **22**(2): p. 892-897.
- 517 28. Chen, Y., S. Mori, and W.-P. Pan, Studying the mechanisms of ignition of coal particles by TG-DTA.  
518 *Thermochimica Acta*, 1996. **275**(1): p. 149-158.
- 519 29. Fang, X., L. Jia, and L. Yin, A weighted average global process model based on two- stage kinetic scheme  
520 for biomass combustion. *Biomass and Bioenergy*, 2013. **48**: p. 43-50.
- 521 30. Wang, G., et al., Characterisation and model fitting kinetic analysis of coal/biomass co-combustion.  
522 *Thermochimica Acta*, 2014. **591**: p. 68-74.
- 523 31. Gil, M.V., et al., Thermal behaviour and kinetics of coal/biomass blends during co-combustion. *Bioresource*  
524 *Technology*, 2010. **101**(14): p. 5601-5608.
- 525 32. Shen, D., et al., Kinetic study on thermal decomposition of woods in oxidative environment. *Fuel*, 2009.  
526 **88**(6): p. 1024-1030.
- 527 33. Shi, H., Kinetic study of fire combustible pyrolysis. Zhejiang University, Hangzhou, 2004: p. 20-21.
- 528 34. Kai, X., et al. The effect of biomass components on the co-combustion characteristics of biomass with coal.  
529 in *Digital Manufacturing and Automation (ICDMA)*, 2011 Second International Conference on. 2011. IEEE.
- 530 35. Li, Y. and D. Drysdale, Measurement of the ignition temperature of wood. *Fire Safety Science*, 1992. **1**: p.  
531 380-385.
- 532 36. López-González, D., et al., Thermogravimetric-mass spectrometric analysis on combustion of lignocellulosic  
533 biomass. *Bioresource technology*, 2013. **143**: p. 562-574.
- 534 37. Cheng, K., W.T. Winter, and A.J. Stipanovic, A modulated-TGA approach to the kinetics of lignocellulosic  
535 biomass pyrolysis/combustion. *Polymer Degradation and Stability*, 2012. **97**(9): p. 1606-1615.
- 536 38. Khan, M.M., J.L. De Ris, and S.D. Ogden, Effect of moisture on ignition time of cellulosic materials. *Fire*  
537 *Safety Science*, 2008. **9**: p. 167-178.
- 538 39. Atreya, A. and M. Abu-Zaid, Effect of environmental variables on piloted ignition. *Fire Safety Science*,  
539 1991. **3**: p. 177-186.
- 540 40. Moghtaderi, B., et al., A new correlation for bench-scale piloted ignition data of wood. *Fire safety journal*,  
541 1997. **29**(1): p. 41-59.
- 542 41. Sorek, N., et al., The implications of lignocellulosic biomass chemical composition for the production of  
543 advanced biofuels. *BioScience*, 2014. **64**(3): p. 192-201.

- 544 42. Milosavljevic, I. and E.M. Suuberg, Cellulose thermal decomposition kinetics: global mass loss kinetics.  
545 Industrial & Engineering Chemistry Research, 1995. **34**(4): p. 1081-1091.
- 546 43. Álvarez, A., et al., Determination of kinetic parameters for biomass combustion. Bioresource technology,  
547 2016. **216**: p. 36-43.
- 548 44. Wang, S., et al., Combustion characteristics of seaweed biomass. 1. Combustion characteristics of  
549 Enteromorpha clathrata and Sargassum natans. Energy & Fuels, 2009. **23**(10): p. 5173-5178.
- 550 45. Hosoya, T., H. Kawamoto, and S. Saka, Cellulose–hemicellulose and cellulose–lignin interactions in wood  
551 pyrolysis at gasification temperature. Journal of analytical and applied pyrolysis, 2007. **80**(1): p. 118-125.
- 552 46. Zhang, J., et al., Cellulose–hemicellulose and cellulose–lignin interactions during fast pyrolysis. ACS  
553 Sustainable Chemistry & Engineering, 2015. **3**(2): p. 293-301.
- 554 47. Jin, Z., et al., Covalent linkages between cellulose and lignin in cell walls of coniferous and nonconiferous  
555 woods. Biopolymers, 2006. **83**(2): p. 103-110.
- 556 48. Garcia-Maraver, A., et al., Determination and comparison of combustion kinetics parameters of agricultural  
557 biomass from olive trees. Renewable Energy, 2015. **83**: p. 897-904.

**Highlights**

- First research on biomass ignition through its chemical compounds was conducted.
- Ignition temperatures of cellulose, hemicellulose and lignin were determined.
- The effects of interaction of biomass compounds on its ignition were negligible.
- Ignition temperature of biomass is predictable via its chemical compounds.